

## Accepted Article

**Title:** Egyptian grave goods of Kha and Merit studied by neutron and gamma techniques.

**Authors:** Giulia Festa, Triestino Minniti, Laura Arcidiacono, Matilde Borla, Daniela Di Martino, Federica Facchetti, Enrico Ferraris, Valentina Turina, Winfried Kockelmann, Joe Kelleher, Roberto Senesi, Christian Greco, and Carla Andreani

This manuscript has been accepted after peer review and appears as an Accepted Article online prior to editing, proofing, and formal publication of the final Version of Record (VoR). This work is currently citable by using the Digital Object Identifier (DOI) given below. The VoR will be published online in Early View as soon as possible and may be different to this Accepted Article as a result of editing. Readers should obtain the VoR from the journal website shown below when it is published to ensure accuracy of information. The authors are responsible for the content of this Accepted Article.

**To be cited as:** *Angew. Chem. Int. Ed.* 10.1002/anie.201713043  
*Angew. Chem.* 10.1002/ange.201713043

**Link to VoR:** <http://dx.doi.org/10.1002/anie.201713043>  
<http://dx.doi.org/10.1002/ange.201713043>

## Egyptian grave goods of Kha and Merit studied by neutron and gamma techniques.

G. Festa<sup>[a]\*</sup>, T. Minniti<sup>[b]\*</sup>, L. Arcidiacono<sup>[a,c]</sup>, M. Borla<sup>[d]</sup>, D. Di Martino<sup>[e]</sup>, F. Facchetti<sup>[f]</sup>, E. Ferraris<sup>[f]</sup>, V. Turina<sup>[f]</sup>, W. Kockelmann<sup>[b]</sup>, J. Kelleher<sup>[b]</sup>, R. Senesi<sup>[g,a,h]</sup>, C. Greco<sup>[f]</sup>, C. Andreani<sup>[g,a,h]</sup>

**Abstract:** Artifacts from the Egyptian grave goods of *Kha* and *Merit* preserved at the Museo Egizio in Turin, have been studied through a synergic combination of non-destructive and non-invasive neutron and gamma techniques (namely neutron imaging, neutron diffraction and Prompt Gamma Activation Analysis). Results provide unprecedented morphological reconstructions of the inner parts of the two alabaster and metallic vases, their isotopic and phase composition, extending our knowledge of hitherto unknown content of the vases and their functions.

This paper presents a non-destructive and non-invasive study of ancient Egyptian objects from the grave-goods of “*Kha and Merit*” preserved at the *Museo Egizio* in Turin. A synergic combination of neutron and gamma techniques were employed at the ISIS pulsed neutron source (UK). The intact burial assemblage, discovered at *Deir el-Medina (Luxor, West Bank)*, belonged to upper-class individuals: the ‘Overseer Director’ *Kha* and his wife *Merit*<sup>[1,2]</sup>. It represents the richest and most complete non-royal burial assemblage ever found and housed in a museum outside Egypt; this collection dates back to the New Kingdom (1425–1353 BC). Well after the first application in 1896,<sup>[3]</sup> today chemical–physical techniques are routinely used for the analysis of objects in the field of archaeological science. Here, neutron techniques were applied to the study of a sealed alabaster vase and a metallic situla from the *Kha and Merit* grave goods. The main goal of the investigation of the alabaster vase was to image its content without unsealing it; the analysis of the metallic situla aimed to analyze metal compositions and manufacturing technologies. The alabaster vase is part of a set of seven sealed alabaster containers, which were found in a closed box, secured by the Egyptians with special care. It has been suggested that these could be the famous Seven Sacred Oils, known only in literature and never actually discovered. High-resolution Neutron Radiography (NR) and Neutron Tomography (NT), Prompt

Gamma Activation Analysis (PGAA), and Neutron Diffraction (ND) were employed in the present study. The experiment was carried out at the Imaging and Materials Science & Engineering (IMAT) beamline<sup>[4–6]</sup> for NR, NT and PGAA measurements and at the ENGIN-X<sup>[7–9]</sup> beamline for ND measurements; both are located at ISIS Pulsed Neutron Source, UK. The schematic set-up for the measurements is shown in figure 1.

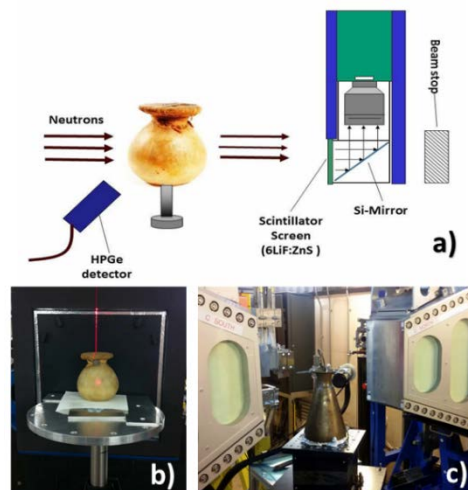


**Figure 1.** a) Schematic layout of the experimental setup. Photographs of the setup at b) IMAT beamline for PGAA, NR and NT. c) at ENGIN-X beamline for ND.

Normalized radiographies were performed on both objects, as shown in figure 2. NT was carried out to understand the internal morphology of the alabaster vase.



**Figure 2.** a) Photo of the alabaster sealed vase (S.8442) and its neutron radiography, b) Photo of the metallic situla (S.8228) and its neutron radiography. The alabaster vase is 11cm height and 10cm of max. diameter while the metallic situla is 26cm height and 16cm of max. diameter.

Correspondence: [giulia.festa@centrofermi.it](mailto:giulia.festa@centrofermi.it), [triestino.minniti@stfc.ac.uk](mailto:triestino.minniti@stfc.ac.uk)

[a] Centro Fermi - Museo Storico della Fisica e Centro Studi e Ricerche “Enrico Fermi”, It

[b] STFC, Rutherford Appleton Laboratory, ISIS Facility, UK

[c] UCL, Institute of Archaeology, UK

[d] Soprintendenza Archeologia, Belle Arti e Paesaggio per la Città Metropolitana di Torino, It

[e] Università degli Studi di Milano-Bicocca, Dip. Fisica, It

[f] Museo Egizio di Torino, It

[g] Università degli Studi di Roma Tor Vergata, Dip. Fisica and NAST Centre, It

[h] CNR – Istituto per i Processi Chimico-Fisici (IPCF), It

## COMMUNICATION

In figure 3, NT slices<sup>[10]</sup> and 3D volume rendering of the alabaster vase are shown. The content is an almost homogeneous substance, which strongly attenuates the incident neutron beam. Furthermore, the image unveils the presence of a truncated-cone plug under the linen sheets (figure 3d). The inner material has an average neutron transmission of  $T=1.6\%$  while the outer region of  $T=11\%$ . The radiographies of the bronze-based metallic situla (figure 2b) were combined in a single normalized NR, via the MOSAICJ<sup>[11]</sup> plugin of the IMAGEJ<sup>[12]</sup>. The situla is composed of two pieces held together by rivets and the upper part is opaque to neutrons. Such effect can be attributed to thicker vase walls or to elements with higher neutron attenuation (i.e. organic residues). CT of the alabaster vase was obtained both through Simultaneous Algebraic Reconstruction Technique (SART) algorithm and standard Filtered Back-Projection (FBP) algorithm using OCTOPUS.<sup>[13]</sup> Comparison between the Signal to Noise Ratio (SNR) and the Contrast to Noise Ratio (CNR)<sup>[14]</sup> for both algorithms, was carried out and is presented in figures 3a and b. The CT reconstruction via SART algorithm (SNR $\approx$ 33 and CNR $\approx$ 62) produced better results compared to the FBP algorithm (SNR $\approx$ 29 and CNR $\approx$ 52) and was applied in the present case. Volume rendering and segmentation of the vase, through VGSTUDIO MAX<sup>[15]</sup>, is shown in figure 3c. In figure 3d a virtual cross-section of the vase is also shown.

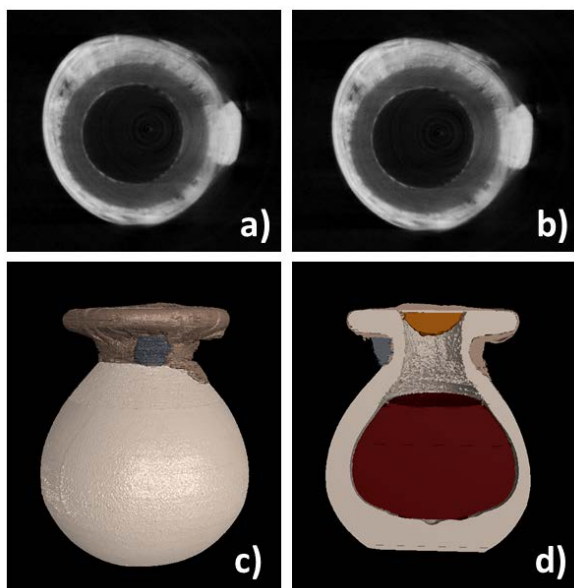


**Figure 3.** NT sections of the alabaster vase (S.8442): a) CT slice obtained by FBP algorithm; b) CT slice obtained by SART algorithm; c) volume rendering of the vase, results of the segmentation process d) NT virtual slicing of the vase. Dimensions of the voxel are  $0.103 \text{ mm}^3$ .

The truncated cone geometry of the plug (orange in figure 3d) has a base radius of about 1.5cm and a height of 1.2cm for a total volume of about  $4 \text{ cm}^3$ : its linear attenuation coefficient  $\Sigma$ , obtained through the procedure described in ref.<sup>[16]</sup> is  $\Sigma_{\text{plug}}=(3.06\pm 0.01) \text{ cm}^{-1}$ . Experimental and predicted  $\Sigma$  for segmented portions are reported in Table 1. The  $\Sigma$  of the plug is similar to the coefficient obtained for the alabaster,  $\Sigma_{\text{vase}}$

$\text{body}=(3.27\pm 0.01) \text{ cm}^{-1}$  (orange in figure 3d) demonstrating that the plug is made of alabaster. Experimental  $\Sigma$  for alabaster (body and plug) is compared with the predicted value for the same material ( $\Sigma_{\text{plug}}=(3.10\pm 0.01) \text{ cm}^{-1}$ ), as calculated from a density of  $2.7 \text{ g/cm}^3$ , and for a  $\lambda = 2.6 \text{ \AA}$ , for IMAT.<sup>[17]</sup> A similar analysis was carried out for linen strips (dark beige in figure 3c and d); here, the measured coefficient is  $\Sigma_{\text{linen}}=(4.23\pm 0.01) \text{ cm}^{-1}$ . The internal content of the vase (dark red in figure 3d) shows an absorption coefficient compatible with an organic compound such as a mixture of oils and wax.<sup>[18-20]</sup> For comparison purposes, a mixture of typical animal and vegetal organic compounds was considered to predict neutron linear attenuation coefficient as reported in Table 1. As a result, values are higher compared to the measured attenuation coefficient of the vase's content. Such difference is attributed to density reduction due to evaporation and condensation processes. The best match with the predicted  $\Sigma$  is obtained with a density reduction in the range of 20-23%.

**Table 1.** List of the main components of the alabaster vase with chemical composition and density, used for the estimation of the predicted  $\Sigma$  for thermal neutrons.

Component	Predicted chemical composition	Density ( $\text{g/cm}^3$ ) at room temperature	Volume ( $\text{cm}^3$ )	$\Sigma_{\text{measured}}$ ( $\text{cm}^{-1}$ )	$\Sigma_{\text{predicted}}$ ( $\text{cm}^{-1}$ ) @ 2.6 Å
Vase body	Alabaster <sup>[18]</sup>	2.7 <sup>[18]</sup>	363.8	3.27	3.10
Plug	Alabaster <sup>[18]</sup>	2.7 <sup>[18]</sup>	4.0	3.06	3.10
Linen textile	Cellulose (92%) Lignin (4%)	1.5 <sup>[19]</sup>	22.0	4.23	4.47
Olive oil <sup>[20]</sup>	Palmitic acid (8-18%) Stearic acid (2-5%) Oleic acid (56-82%) Linoleic acid (4-19%) Linolenic acid (0.3-1%)	0.852 0.941 0.895 0.900 0.916	232.4	3.96	5.24 3.96@76%
Linseed oil <sup>[20]</sup>	Palmitic acid (6-7%) Stearic acid (3-6%) Oleic acid (14-24%) Linoleic acid (14-19%) Linolenic acid (48-60%)	0.852 0.941 0.895 0.900 0.916	232.4	3.96	5.13 3.96@77%
Pig fat <sup>[20]</sup>	Myristic acid (1-2%) Palmitic acid (20-28%) Stearic acid (13-16%) Oleic acid 42-45%) Linoleic acid (8-10%) Linolenic acid (0.5-2%)	0.990 0.852 0.941 0.895 0.900 0.916	232.4	3.96	4.90 3.96@80%
Beef tallow <sup>[20]</sup>	Myristic acid (2-3%) Palmitic acid (23-30%) Stearic acid (14-29%) Oleic acid (40-50%) Linoleic acid (1-3%) Linolenic acid (0-1%)	0.990 0.852 0.941 0.895 0.900 0.916	232.4	3.96	5.23 3.96@76%

A PGAA<sup>[21,22]</sup> movable set-up was used for isotopic and elemental analysis of the two artifacts. PGAA spectra (shown in figure 4, and the relative percentages of the detected isotopes reported in table 2), were obtained through the normalization procedure reported in ref.<sup>[21]</sup>. The main elements detected from the alabaster vase and its internal content are Mg, S, O, Ca and C; C and O may be connected to the presence of organic oils and resins inside the vase, while Mg, S and Ca are interpreted as part of the alabaster. It should be noted that Fe is lower than the detection limits of PGAA on IMAT due to the high background signal.<sup>[21]</sup> The upper part of the situla, where a region up to 10 cm from the top neck of the vase was irradiated, presents a dark coating on one side, which is labeled by archaeologists as possible bitumen. Additionally, PGAA was carried out on the bottom area with an exposed beam region up to 16 cm from the bottom edge of the vase during radiography.

COMMUNICATION

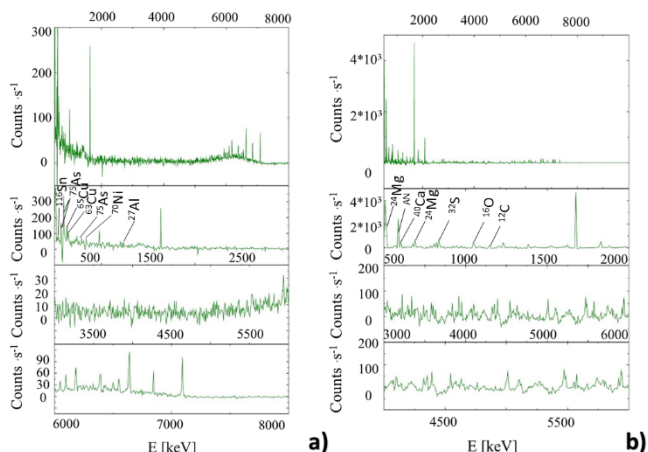


**Figure 4.** a) Prompt  $\gamma$ -ray spectrum of the situla (S.8228), upper region, recorded at the IMAT beamline; b) Prompt  $\gamma$ -ray spectrum of the Alabaster vase (S.8442). The three lower panels in figure a) and b) provide the expanded view of the collected spectra.

A comparison between PGAA spectra of the situla, shows that the upper region presents additional peaks associated with the presence of Ni, V and N, which are identified as a bitumen component.<sup>[22-24]</sup>

**Table 2.** Results from PGAA elemental/isotopic analysis. The errors are  $\pm 0.001\%$ .

SEALED ALABASTER VASE								
	<sup>24</sup> Mg	<sup>32</sup> S	<sup>12</sup> C	<sup>40</sup> Ca	<sup>16</sup> O			
%	0,073	2,700	0,045	100	0,005			
METALLIC SITULA								
	<sup>75</sup> As	<sup>63</sup> Cu	<sup>65</sup> Cu	<sup>27</sup> Al	<sup>116</sup> Sn	<sup>60</sup> Ni	<sup>51</sup> V	<sup>14</sup> N
Lower part %	0,300	100		0,020	1,280			
Upper part %	0,040	100		0,590	12,400	0,024	0,001	0,350

The metallic situla was studied through spatially resolved ND with a gauge volume of  $2 \times 2 \times 2 \text{ mm}^3$ . Figure 5 shows ND spectra of the situla. Results of the quantitative analysis were carried out via GSAS<sup>[25,26]</sup>, based on the Rietveld refinement method<sup>[27]</sup> and are reported in Table 3. The Sn contents were calculated via Vegard's rule assuming a binary Cu-Sn bronze.<sup>[6]</sup> The estimated standard deviation (e.s.d.) for single point lattice parameters is much smaller than the variability between points of the same series. The latter translates into a variation of the equivalent Sn-content of 0.2wt%. The e.s.d of the phase fraction values is about 1%. A diffraction peak broadening parameter was refined with the data, and compared to the instrumental width of ENGIN-X.

**Table 3.** Results from Neutron Diffraction on the metallic situla. Average lattice parameters for S1-S8. The errors on lattice parameters are  $\pm 0.0001\%$ .

	Lattice parameter (Å)		Phase Fractions		Sn content [wt%]	
	Copper Alloy 1 (Å)	Copper Alloy 2 (Å)	Copper Alloy 1 (wt%)	Copper Alloy 2 (wt%)	Sn % in Alloy 1 (wt%)	Sn % in Alloy 2 (wt%)
S1	3.6253	-	100	-	1.9	-
S2	3.6246	-	100	-	1.8	-
S3	3.6254	3.6673	60*	40**	1.9	9.6
S4	-	3.6649	100	-	-	9.1
S5	-	3.6652	-	100	-	9.2
S6	-	3.6640	-	100	-	9.0
S7	3.6196	3.6600	93	7	0.9	8.4

S8	3.6526	-	100	-	6.9	-
----	--------	---	-----	---	-----	---

Diffraction scans showed that the situla is composed of parts with distinct bronze alloys. The lower part is made of a low tin bronze with about 2% Sn whereas the upper part is made of a 9% Sn bronze. The peak widths of both alloys are significantly broadened but the peak shape is fairly smooth. Both observations are indicative of a cold-worked material with remnants of cored dendrites. The data from the neck (S6) yield the same high-tin bronze, but the alloy was not homogenized. In comparison, the peaks from the hinge support attached to the rim are broadened due to dendritic segregation, present in as-cast alloy. The hinge support is made of a 9% Sn bronze whereas the rim itself is made of a 1% Sn bronze. The handle is made of a copper alloy, which appears slightly reduced in Sn (7%). The S3 scan shows that the rivets are made of the same low-Sn copper alloy of the lower region.<sup>[28]</sup> It should be noted that diffraction and PGAA results are in agreement.

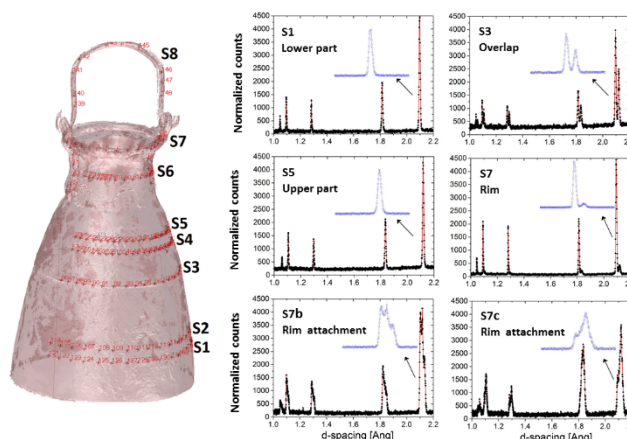


**Figure 5.** Comparison of diffraction patterns from different parts of the situla in the d-spacing range 1 – 2.2 Å, with the (111) bronze peak shape highlighted in the inset. The location of analysis point series are indicated on the laser-surface scan of the situla.

In conclusion, the synergic combination of neutron techniques enabled to unveil information about two ancient Egyptian artifacts preserved at the *Museo Egizio* in Turin. The results show unprecedented data about the inner morphology, structure and elemental composition of both complex vases. The sealed alabaster vase is filled with organic material and presents an alabaster cone-shape plug covered with linen stripes. The situla is made of different alloys and composed of two halves joined together by rivets, made of the same alloy as the lower part. The applied experimental methods employed in this study are expected to have further impact across several disciplines, from materials and environmental science, to paleontology and archaeology. Analyses of alabaster, textiles and wood artifacts from the same grave are currently in progress.

Accepted Manuscript

## Acknowledgements

This research is supported by CNR, within the CNR-STFC Agreement 2014–2020 (N. 3420), concerning collaboration in scientific research at the ISIS Spallation Neutron Source, and by the ARKHA project<sup>[29]</sup>.

**Keywords:** neutron tomography • prompt gamma activation analysis • neutron diffraction • Egyptian

- 
- [1] E. Schiaparelli, *Relazione sui lavori della Missione Archeologica Italiana in Egitto (anni 1903-1920). Vol. II, La tomba intatta dell'architetto Kha nella necropoli di Tebe*, (Turin 1927), A. Roccati, Turin 2007.
- [2] E. Ferraris, *La tomba di Kha*, in AA.VV., *Museo Egizio*, pp. 130-151, Modena 2015.
- [3] J. Taylor, University of Texas Press, 1996, 72.
- [4] T. Minniti et al., *J. Instrum.*, 2016, 11, C03014.
- [5] W. Kockelmann, et al., *Phys. Procedia*, 2015, 69, 71.
- [6] V. Finocchiaro et al., *Rev. Sci. Instrum.*, 2013, 84, 093701.
- [7] J. R. Santisteban et al., *J Appl Cryst.*, 2006, 39, 812.
- [8] S. Siano et al., *Archaeometry*, 2006, 48, 1, 77.
- [9] G. Festa et al., *J. of Appl. Phys.*, 2011, 109-6.
- [10] A. C. Kak and M. Slaney Malcolm Slaney, 1999, IEEE press.
- [11] P. Thévenaz, M. Unser, *Micr. Res. and Tech.*, 2007, 70(2), 135-146.
- [12] J. Schindelin, I. Arganda-Carreras & F. Frise, *Nature methods*, 2012, 9(7), 676-682.15.  
<https://www.octopusimaging.eu/>
- [13] M. Welvaert, Y. Rosseel, *PLoS ONE*, 2013, 8(11): e77089.
- [14] <https://www.volumegraphics.com/en/products/vgstudio-max.html>
- [15] R. Van Langh et al., *Anal Bioanal Chem*, 2009, 395:1949–1959.
- [16] W. Kockelmann et al., *Journal of Imaging*, 2018, 4, 47.
- [17] A. Frumkin et al., *J. of Arch. Science*, 2014, 41, 749.
- [18] A. Amiri et al. "Standard density measurement method development for flax fiber", In *Industrial Crops and Products*, 2017, 96, 196.
- [19] M. Serpico and R. White, 'Oil, fat and wax' in P.T. Nicholson, I. Shaw 'Ancient Egyptian Materials and Technology', Cambridge University Press 2000.
- [20] G. Festa et al., *J. of Instr.*, 2017, 12 P08005.
- [21] J. A. Harrell, *Bitumen, ancient Egypt*, The encyclopedia od Ancient History, 2013.
- [22] M. L. Proefke et al., *Anal. chem.*, 1992, 64-2.
- [23] K. A. Clark, S. Ikram and R. P. Evershed, *Phil. Trans R. Soc. A*, 2016, 374: 20160229.
- [24] A.C. Larson and R.B. Von Dreele, Los Alamos National Laboratory Report, LAUR 86-748.
- [25] B. Toby, *J. Appl. Cryst.* 34, 2001, 210-3.
- [26] R.J. Hill and C.J. Howard, *J. Appl. Cryst.*, 1987, 20, 467–74.
- [27] D.A. Scott, 'Copper and Bronze in Art', Getty Conservation Institute, Los Angeles, 2002.
- [28] C. Andreani et al., *J. Anal. At. Spectrom.*, 2017, 32, 1342-1347.
- [29]